

Accepted Manuscript

A novel method combining additive manufacturing and alloy infiltration for NdFeB bonded magnet fabrication

Ling Li, Angelica Tirado, B.S. Conner, Miaofang Chi, Amy M. Elliott, Orlando Rios, Haidong Zhou, M. Parans Paranthaman

PII: S0304-8853(16)32346-0

DOI: <http://dx.doi.org/10.1016/j.jmmm.2017.04.066>

Reference: MAGMA 62670

To appear in: *Journal of Magnetism and Magnetic Materials*

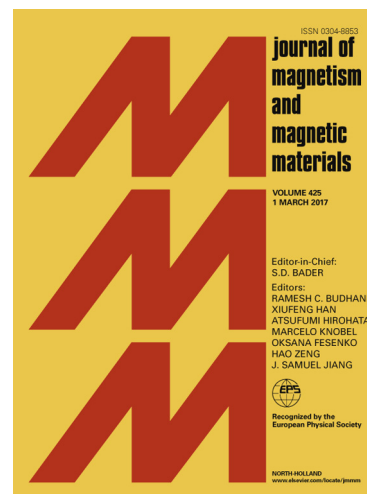
Received Date: 25 September 2016

Revised Date: 17 January 2017

Accepted Date: 15 April 2017

Please cite this article as: L. Li, A. Tirado, B.S. Conner, M. Chi, A.M. Elliott, O. Rios, H. Zhou, M.P. Paranthaman, A novel method combining additive manufacturing and alloy infiltration for NdFeB bonded magnet fabrication, *Journal of Magnetism and Magnetic Materials* (2017), doi: <http://dx.doi.org/10.1016/j.jmmm.2017.04.066>

This is a PDF file of an unedited manuscript that has been accepted for publication. As a service to our customers we are providing this early version of the manuscript. The manuscript will undergo copyediting, typesetting, and review of the resulting proof before it is published in its final form. Please note that during the production process errors may be discovered which could affect the content, and all legal disclaimers that apply to the journal pertain.



A novel method combining additive manufacturing and alloy infiltration for NdFeB bonded magnet fabrication

Ling Li¹, Angelica Tirado¹, B. S. Conner², Miaofang Chi³, Amy M. Elliott⁴, Orlando Rios², Haidong Zhou⁵, M. Parans Paranthaman^{1,*}

¹⁾ *Chemical Sciences Division, Oak Ridge National Laboratory, Oak Ridge, TN 37831, USA*

²⁾ *Materials Science and Technology Division, Oak Ridge National Laboratory, Oak Ridge, TN 37831, USA*

³⁾ *Center for Nanophase Materials Sciences, Oak Ridge National Laboratory, Oak Ridge, TN 37831, USA*

⁴⁾ *Manufacturing Demonstration Facility, Oak Ridge National Laboratory, Tennessee, 37932, USA*

⁵⁾ *Department of Physics and Astronomy, University of Tennessee, Knoxville, Tennessee 37996, USA*

Abstract

In this paper, binder jetting additive manufacturing technique is employed to fabricate NdFeB isotropic bonded magnets, followed by an infiltration process with low-melting point eutectic alloys [i.e., Nd₃Cu_{0.25}Co_{0.75} (NdCuCo) and Pr₃Cu_{0.25}Co_{0.75} (PrCuCo)]. Densification and mechanical strength improvement are achieved for the as-printed porous part. Meanwhile, the intrinsic coercivity H_{ci} is enhanced from 732 to 1345 kA/m and 1233 kA/m after diffusion of NdCuCo and PrCuCo, respectively. This study presents a novel method for fabricating complex-shaped bonded magnets with promising mechanical and magnetic properties.

Corresponding author: paranthamanm@ornl.gov

Keywords: Additive manufacturing; NdFeB; Bonded magnets; Coercivity; Infiltration.

Introduction

$\text{Nd}_2\text{Fe}_{14}\text{B}$ -based permanent magnets (PMs) exhibit a variety of clean energy applications such as in wind turbines and electric vehicles [1]. One well-known concern about these strong PMs is their dependency on critical materials such as rare earths Dy and Nd. Bonded magnets are fabricated by blending magnetic powders with polymer binders, conventionally using injection or compression molding, which gives rise to advantages such as net shape capability, reduced waste, and mechanical flexibility, *etc* [2]. Even though the energy product $(\text{BH})_{\text{max}}$ is sacrificed as it is proportional to the square of the loading fraction of the magnet powder in the binder, bonded magnets can still alleviate rare earths criticality in certain applications. Additive manufacturing (AM) enables rapid production with no tooling required and minimum materials waste, offering an economical procedure for producing permanent magnets which heavily contains rare earth elements [3, 4]. We have recently demonstrated the successful fabrication of NdFeB bonded magnets using binder jetting AM technique [5]. However, the as-printed magnets are porous, and possess relatively low density and low mechanical strength. Infiltration through bronze is a common post-processing stage (annealing at 1050 °C in flowing argon) to enhance the mechanical strength of the binder jet printed part (*e.g.*, stainless steel) while retaining the complex shape. Therefore, bronze infiltration was done in this study to the binder jetted NdFeB magnets, nevertheless, resulting in chemical phase decomposition to soft α -Fe as confirmed by x-ray diffraction, thus loss of coercivity.

In the field of permanent magnetism, much efforts have been devoted to improving the high temperature applications of NdFeB because its coercivity and energy product degrades rapidly with increasing temperature. One well-established method is to diffuse the starting powders with Dy [6], which enhances the coercivity through increasing the magnetic anisotropy [7]. Nevertheless, the magnetic moments of Dy couples with that of Fe antiferromagnetically, leading to the reduction in net magnetization [7]. Furthermore, Dy is defined as the most critical element [8]. To solve this problem, a great deal of research has been focused on enhancing the coercivity of NdFeB through grain boundary infiltration with Dy free alloys. For example, grain boundary diffusion process (GBDP) using low-melting point eutectic alloys (*i.e.*, Nd-Cu, Pr-Cu, Pr-Cu-Co, *etc.*) has been widely utilized to enhance the intrinsic coercivity in melt-spun nanocrystalline ribbons [9], sintered magnets [10-14], hydrogenation-disproportionation-desorption-recombination (HDDR) powders [15, 16], and thin films [17]. It is generally believed that a thick

rare earth rich and iron deficient phase is essential in weakening the exchange coupling between $\text{Nd}_2\text{Fe}_{14}\text{B}$ grains, resulting in enhanced coercivity.

Therefore, it is of interest to infiltrate the as binder jetted magnets with low-melting point eutectic alloys to achieve physically and magnetically stronger parts with net shape capability. In this paper, bonded NdFeB magnets are first 3D printed via binder jetting, and then infiltrated with two low-melting point alloys with nominal compositions of $\text{Nd}_3\text{Cu}_{0.25}\text{Co}_{0.75}$ (NdCuCo) and $\text{Pr}_3\text{Cu}_{0.25}\text{Co}_{0.75}$ (PrCuCo). Densification, mechanical strength improvement, and a significant enhancement in the intrinsic coercivity are achieved. Microstructural observations support the generally accepted magnetic isolation mechanism responsible for coercivity enhancement. Namely, the excess non-ferromagnetic Nd/Pr rich and Fe deficient phase isolates the magnetic $\text{Nd}_2\text{Fe}_{14}\text{B}$ grains, which likely hinders the exchange coupling between the magnetic grains and suppresses the nucleation of reversal grains.

Methods

A binder jetting additive manufacturing process was employed to 3D print the NdFeB bonded magnet using an ExOne X1-Lab printer as described in detail previously [5]. The powder used for printing is a resin-coated isotropic NdFeB powder (Magnequench, MQP-B-20173-070) with an average diameter of 70 μm . Aqueous solutions of Diethylene Glycol (DEG) were used as the binder. The intrinsic coercivity H_{ci} of the starting powder is 732 kA/m. The as-printed pieces were then placed in an oven at 150 °C for 2 h to cure the binder. The cured magnets were shaped to rectangular, and the density was determined to be 3.3 g/cm³, which is approximately 43% relative to the NdFeB single crystal density of 7.6 g/cm³. Around 2mm thick binder-jetted magnets were used for the infiltration; then, the inner part of the infiltrated samples was taken for density measurement using the Archimedes' method. Two alloys with nominal compositions $\text{Nd}_3\text{Cu}_{0.25}\text{Co}_{0.75}$ (NdCuCo) and $\text{Pr}_3\text{Cu}_{0.25}\text{Co}_{0.75}$ (PrCuCo) were prepared by arc-melting the elemental metals in stoichiometric ratios. The ingots were re-melted five times to ensure compositional homogeneity. Differential scanning calorimetry (DSC) was performed to determine the melting point of NdCuCo and PrCuCo. The infiltration was carried out in a tube furnace with a flowing argon gas atmosphere at 700°C for 4 h. The alloys were placed on top of the magnets, and then wrapped in tantalum foil with zirconium pieces as oxygen getter in a ceramic crucible boat.

The room temperature magnetization data were collected using a Quantum Design Magnetic Property Measurement System (MPMS) in magnetic fields of up to 4 T. The morphologies of the magnets were examined by backscattered Scanning Electron Microscopy (SEM, Hitachi S-4800). Cross sections of the SEM specimens were polished and carbon coated. Transmission electron microscopy (TEM) characterization was carried out on an aberration-corrected FEI Titan 80/300 microscope. The TEM samples were prepared using a Focused Ion Beam (FIB)/SEM. Energy-dispersive X-ray elemental maps were acquired from the FIB TEM sample with a beam current of 40 pA at room temperature.

Results and Discussion

Fig. 1 shows the DSC curves of the NdCuCo and PrCuCo alloys. It can be seen that both alloys exhibit two phase transitions (*i.e.*, at 510 °C and 601 °C for NdCuCo, 450 °C and 550 °C for PrCuCo), indicating a phase mixture. Fig. 2(a) presents the room temperature magnetization of NdCuCo and PrCuCo *vs.* applied field. The magnetization for both alloys exhibits a linear increase with increasing applied field, indicating a paramagnetic behavior. Fig. 2 (b) exhibits the room temperature demagnetization curves of the as-printed, NdCuCo infiltrated, and PrCuCo infiltrated magnets, all the magnetic characteristics (intrinsic coercivity H_{ci} , remanence B_r , and magnetization at 4T J_{4T}) are shown in Table 1. Note that 1) there is no degradation in intrinsic coercivity H_{ci} in the as-binder jetted magnets as compared to the starting powder; and 2) the magnet experienced a slight volume expansion after the infiltration. A measured average density of 4.3 g/cm³ for the infiltrated samples was used for calculating the polarization J in units of T. The density was improved because the as-printed “green” piece is porous and soft, during the infiltration, the alloys melted and the resulting liquids diffused through the interspaces. Here, the weight ratio of the infiltration alloy to the magnet is ~ 0.46. The intrinsic coercivity of the as-printed sample is enhanced from 732 to 1345 kA/m (~ 83.7 % increase) and 1233 kA/m (~ 68.5 % increase) after diffusion of NdCuCo and PrCuCo, respectively, at an expense of remanence reduction from 0.35 T to 0.31 T (NdCuCo) and 0.25 T (PrCuCo). In addition, the squareness of the hysteresis loop is also degraded after infiltration, which is possibly due to the inhomogeneous coercivity distribution across the magnets [18]. These changes in magnetic characteristics in combination result in a reduced energy product. The reduction in remanence is not unusual [9] as the infiltration alloys are non-ferromagnetic and do not contribute to the net magnetization

(moment per volume of the sample), which is reduced as a result of volume expansion after the infiltration process. In fact, Akiya, *et al.* have found that applying expansion constraint during the GBDP can minimize the remanence reduction via optimizing the volume fraction of the non-ferromagnetic intergranular layer [19]. Furthermore, it was suggested that a possible way to increase the diffusion depth is to apply pressure to create some micro-cracks as diffusion channels [20]. Further work is needed to optimize the infiltration process to gain better control of the uniformity as well as the volume fraction of the non-ferromagnetic phase. It is worth mentioning that annealing the as-printed magnets at 700 °C for 4 h without alloy infiltration caused a significant degradation in coercivity (see Fig. S1), which is due to the chemical phase decomposition to soft α -Fe phase as confirmed by x-ray diffraction (Fig. S2).

To shed light on the mechanism for the coercivity enhancement, the microstructure of the as-printed and infiltrated magnets were examined by backscattered SEM. Fig. 3(a) shows the morphology of the as binder-jetted NdFeB magnet. The magnetic particles in size of 20 to 100 μm are demonstrated as the gray areas in the dark polymer background. Fig. 3(b) and (c) show the backscattered SEM images of the NdCuCo and PrCuCo infiltrated samples. Note that the polymer binder is still present after the infiltration, as evidenced by low magnification SEM images. It can be observed that the alloys (bright areas) are dispersed into the magnetic particles (dark areas), most likely through the cracks, yielding a reduced particle size of below 5 μm after the infiltration.

Fig. 4(a) shows a TEM microstructure image of the NdFeB infiltrated magnet. Fig. 4(b)-(d) present the Energy-dispersive X-ray Spectroscopy (EDS) mapping images of Nd, Fe, and Cu. The darker areas in the mapping image signals element deficiency. It can be observed that for NdCuCo treated samples, the bright areas in Fig.4(a) are Nd, Cu rich and Fe deficient, suggesting that the bright areas mainly consist of the non-ferromagnetic alloys. Similar elemental distributions can be observed in the PrCuCo treated samples, namely the inter-particle phase is Pr rich and Fe deficient, with a small magnetic moment. Two mechanisms controlling coercivity of NdFeB magnets have been proposed: 1) pinning effect; 2) reversal domain nucleation; in both models the high coercivity of NdFeB is related to the phase boundaries between the grains and/or the particles. The coercivity enhancement after infiltration in the present study can be explained as follows. First, the non-ferromagnetic inter-particle phase acts as pinning sites against domain wall motion. Besides, the inter-particle non-ferromagnetic phase impedes demagnetization by

hindering the nucleation and growth of reversal domains. It has been found that the coercivity in sintered NdFeB magnets increases with decreasing Fe content in the intergranular phase, whereby the non-ferromagnetic phase decouples the exchange interaction between neighboring magnetic NdFeB grains [21]. Our microstructural investigations support that the separation of the magnetic particles by the non-ferromagnetic alloys is essential for the improvement of the coercivity in the NdFeB bonded magnets. In addition, previous study revealed that the addition of Co also leads to an enhancement in Curie temperature in NdFeB bonded magnets [22]. Based on that, the addition of Co makes these two low-melting alloys more effective in strengthening the magnetic properties compared to their binary counterparts (i.e., Nd-Cu and Pr-Cu alloys).

Summary

Binder jetting is a novel 3D printing method for fabricating NdFeB bonded magnets. However, the as-printed part suffers from both density and mechanical strength limitations. In this study, a novel method combining binder jetting and alloy infiltration for fabrication of complex-shaped NdFeB bonded magnets is presented. Densification, mechanical strength improvement, and a dramatic enhancement in intrinsic coercivity from 732 to ~ 1300 kA/m are achieved.

Microstructural observations support that the coercivity enhancement is most likely related to the separation of the Nd₂Fe₁₄B magnetic grains induced by the diffusion of the Nd/Pr rich and Fe deficient non-ferromagnetic phase. Low-melting point Dy free alloy diffusion proves to be an effective technique to mechanically strengthen binder jetted bonded magnets, and meanwhile, enhance the coercivity. Optimizations to increase the loading fraction, reduce the porosity, and minimize the remanence reduction and retain the shape during the infiltration process are under way to achieve better properties.

Acknowledgment

This work was supported by the Critical Material Institute, an Energy Innovation Hub funded by the U.S. Department of Energy. The support for AT was provided by the U.S. Department of Energy, Office of Science, Office of Workforce Development for Teachers and Scientists (WDTS) under the Science Undergraduate Laboratory Internship program. The TEM research was supported by the Center for Nanophase Materials Sciences (CNMS), which is sponsored by the Scientific User Facilities Division of the U.S. Department of Energy (DOE), office of Basic

Energy Sciences (BES). L. L. acknowledges Dr. Michael A McGuire for helpful discussions, and Dr. Zhiqian Sun and Dr. Tianyi Chen for helping with the SEM experiments.

Notice: This manuscript has been authored by UT-Battelle, LLC under Contract No. DE-AC05-00OR22725 with the U.S. Department of Energy. The United States Government retains and the publisher, by accepting the article for publication, acknowledges that the United States Government retains a non-exclusive, paid-up, irrevocable, world-wide license to publish or reproduce the published form of this manuscript, or allow others to do so, for United States Government purposes. The Department of Energy will provide public access to these results of federally sponsored research in accordance with the DOE Public Access Plan (<http://energy.gov/downloads/doe-public-access-plan>).

Figure Captions:

Figure 1. DSC curves of the NdCuCo and PrCuCo alloys upon heating from room temperature to 700 °C.

Figure 2. (a) Room temperature magnetization of PrCuCo and NdCuCo; (b) Demagnetization curves of the as binder-jetted, NdCuCo infiltrated, and PrCuCo infiltrated magnets.

Figure 3. Backscattered SEM images of the cross sections of the magnets: (a) as-printed; (b) NdCuCo infiltrated; (c) PrCuCo infiltrated.

Figure 4. (a) TEM image of the NdCuCo infiltrated magnet; (b)-(d) EDS elemental mapping images of Nd, Fe, and Cu, respectively. Note that the mapping was performed within the red squared area.

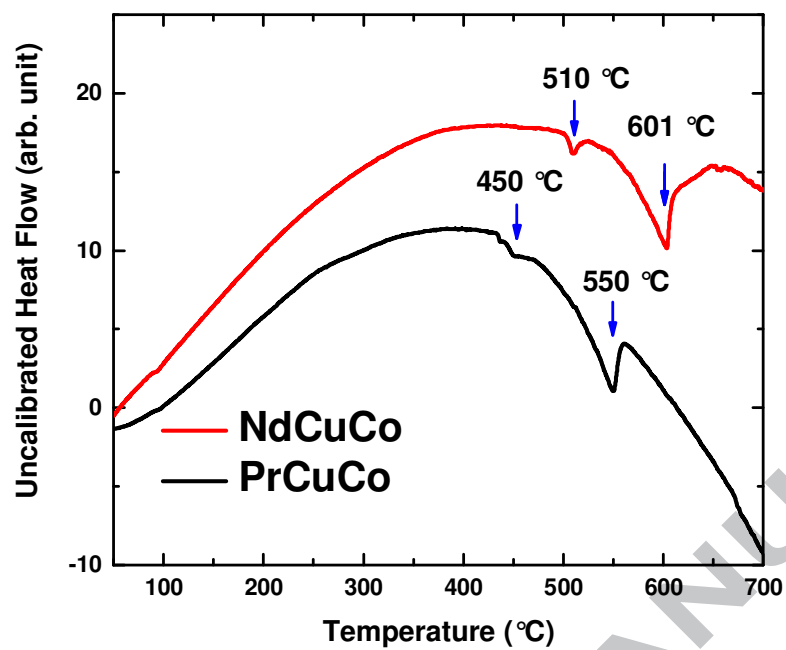


Figure 1. DSC curves of the NdCuCo and PrCuCo alloys upon heating from room temperature to 700 °C.

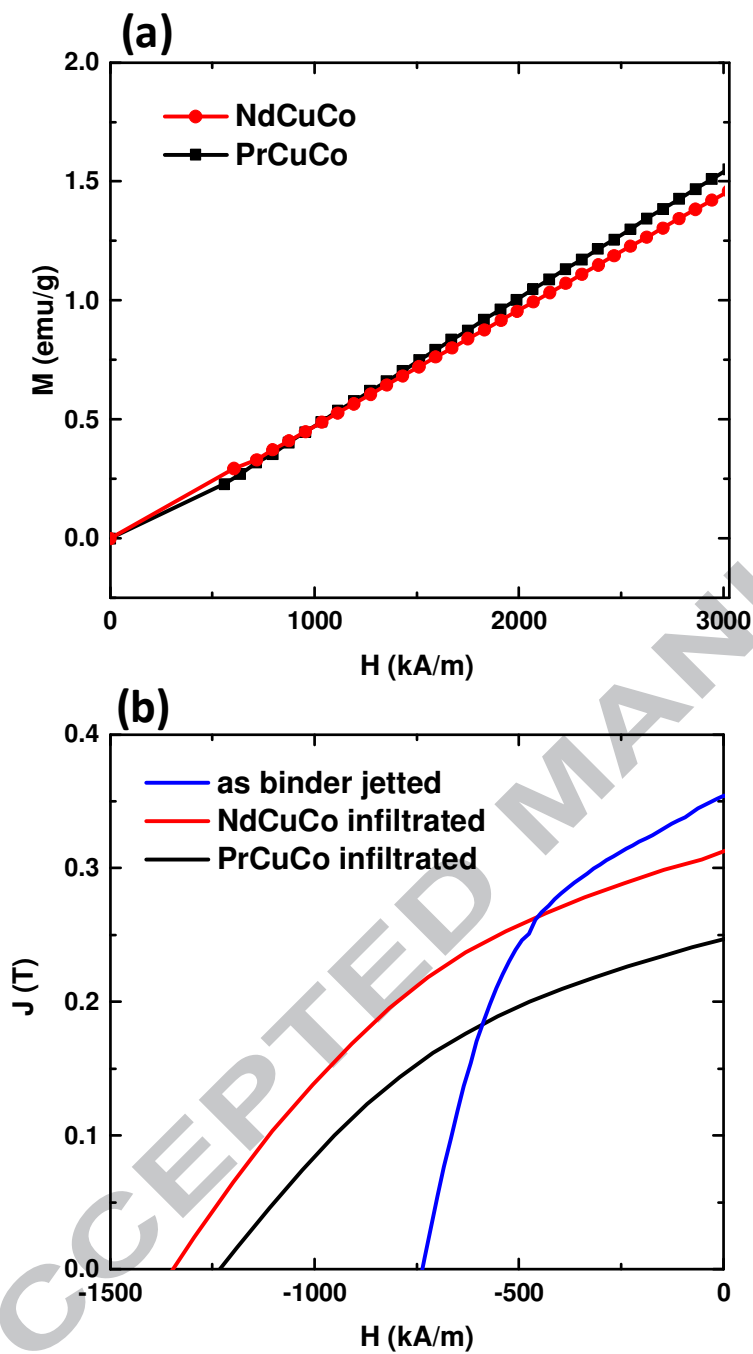


Figure 2. (a) Room temperature magnetization of PrCuCo and NdCuCo; (b) Demagnetization curves of the as binder-jetted, NdCuCo infiltrated, and PrCuCo infiltrated magnets.

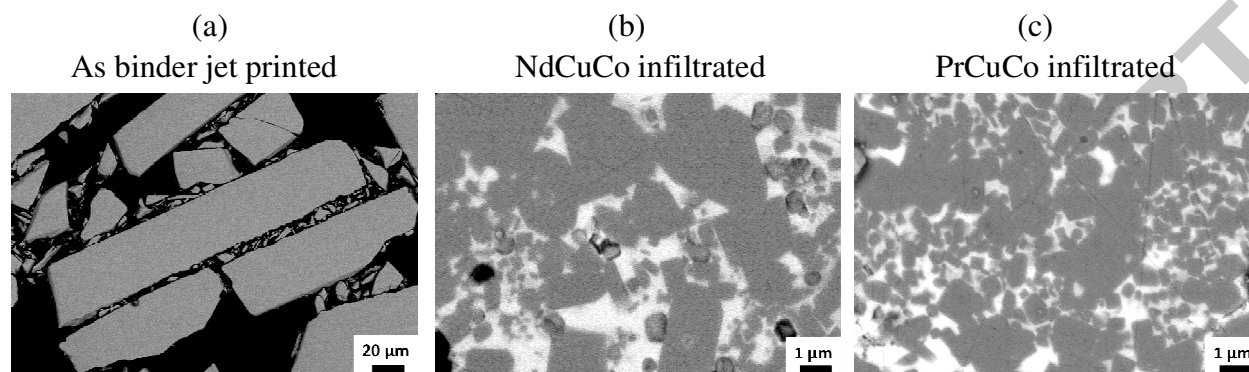


Figure 3. Backscattered SEM images of the cross sections of the magnets (a) as-printed; (b) NdCuCo infiltrated; (c) PrCuCo infiltrated.

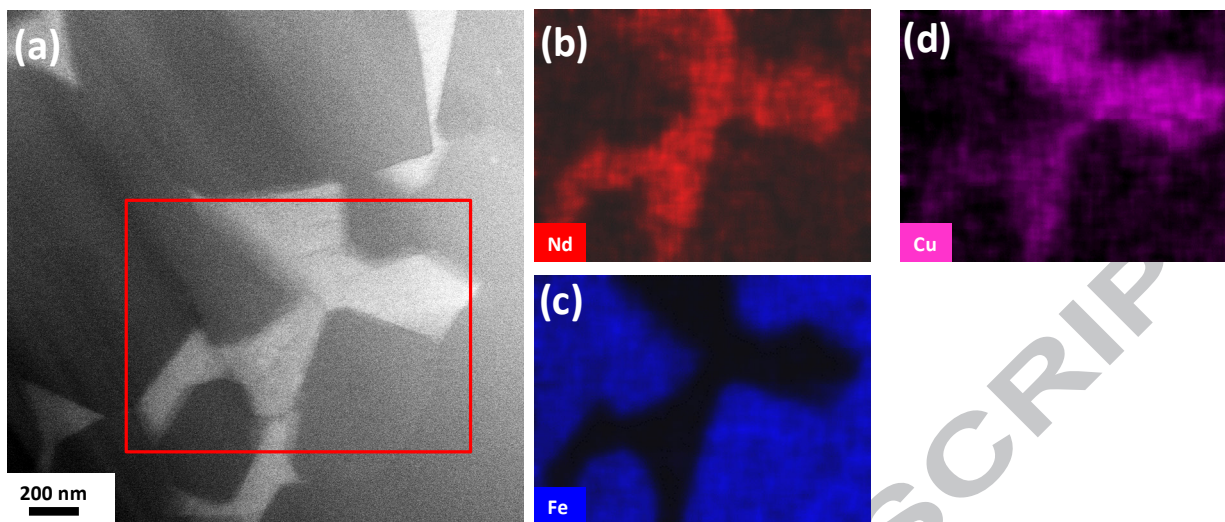


Figure 4. (a) TEM image of the NdCuCo infiltrated magnet; (b)-(d) EDS elemental mapping images of Nd, Fe, and Cu, respectively. Note that the mapping was performed within the red squared area.

Table 1. The density and magnetic properties of the as printed, and NdCuCo, PrCuCo infiltrated magnets.

Sample	Density (g/cm ³)	H_{ci} (kA/m)	B_r (T)	J_{4T} (T)
as printed	3.3	732	0.35	0.53
NdCuCo infiltrated	4.3	1345	0.31	0.50
PrCuCo infiltrated	4.3	1233	0.25	0.39

References

- [1] O. Gutfleisch, M.A. Willard, E. Brück, C.H. Chen, S.G. Sankar, J.P. Liu, Magnetic Materials and Devices for the 21st Century: Stronger, Lighter, and More Energy Efficient, *Adv. Mater.* , 23 (2011) 821-842.
- [2] J. Ormerod, S. Constantinides, Bonded permanent magnets: Current status and future opportunities (invited), *J. Appl. Phys.*, 81 (1997) 4816.
- [3] L. Li, A. Tirado, I.C. Nlebedim, O. Rios, B. Post, V. Kunc, R.R. Lowden, E. Lara-Curzio, R. Fredette, J. Ormerod, T.A. Lograsso, M.P. Paranthaman, Big Area Additive Manufacturing of High Performance Bonded NdFeB Magnets, *Sci. Rep.* , 6 (2016) 36212.
- [4] L. Li, B. Post, V. Kunc, A.M. Elliott, M.P. Paranthaman, Additive manufacturing of near-net-shape bonded magnets: Prospects and challenges, *Scr. Mater.* , (2017).
- [5] M.P. Paranthaman, C.S. Shafer, A.M. Elliott, D.H. Siddel, M.A. McGuire, R.M. Springfield, J. Martin, R. Fredette, J. Ormerod, Binder Jetting: A Novel NdFeB Bonded Magnet Fabrication Process, *JOM*, 68 (2016) 1978-1982.
- [6] N. Hamada, K. Noguchi, C. Mishima, Y. Honkura, Development of anisotropic bonded magnet applied to 150 °C use, *IEEE Trans. Magn.*, 41 (2005) 3847-3849.
- [7] S. Hirose, Y. Matsuura, H. Yamamoto, S. Fujimura, M. Sagawa, H. Yamauchi, Magnetization and magnetic anisotropy of R₂Fe₁₄B measured on single crystals, *J. Appl. Phys.*, 59 (1986) 873-879.
- [8] U.S. Department of Energy. Critical Materials Strategy. Technical report, U.S. Department of Energy. Critical Materials Strategy. Technical report, (2011).
- [9] R. Madugundo, D. Salazar-Jaramillo, J. Manuel Barandiaran, G.C. Hadjipanayis, High coercivity in rare-earth lean nanocomposite magnets by grain boundary infiltration, *J. Magn. Mater.* , 400 (2016) 300-303.
- [10] H. Sepehri-Amin, T. Ohkubo, S. Nagashima, M. Yano, T. Shoji, A. Kato, T. Schrefl, K. Hono, High-coercivity ultrafine-grained anisotropic Nd–Fe–B magnets processed by hot deformation and the Nd–Cu grain boundary diffusion process, *Acta Mater.* , 61 (2013) 6622-6634.
- [11] S. Sawatzki, A. Dirks, B. Frincu, K. Löwe, O. Gutfleisch, Coercivity enhancement in hot-pressed Nd–Fe–B permanent magnets with low melting eutectics, *J. Appl. Phys.* , 115 (2014) 17A705.
- [12] F. Wan, Y. Zhang, J. Han, S. Liu, T. Liu, L. Zhou, J. Fu, D. Zhou, X. Zhang, J. Yang, Y. Yang, J. Chen, Z. Deng, Coercivity enhancement in Dy-free Nd–Fe–B sintered magnets by using Pr–Cu alloy, *J. Appl. Phys.* , 115 (2014) 203910.
- [13] T.G. Woodcock, Q.M. Ramasse, G. Hrkac, T. Shoji, M. Yano, A. Kato, O. Gutfleisch, Atomic-scale features of phase boundaries in hot deformed Nd–Fe–Co–B–Ga magnets infiltrated with a Nd–Cu eutectic liquid, *Acta Mater.* , 77 (2014) 111-124.
- [14] M. Tang, X. Bao, K. Lu, L. Sun, J. Li, X. Gao, Boundary structure modification and magnetic properties enhancement of Nd–Fe–B sintered magnets by diffusing (PrDy)–Cu alloy, *Scr. Mater.* , 117 (2016) 60-63.
- [15] H. Sepehri-Amin, T. Ohkubo, T. Nishiuchi, S. Hirose, K. Hono, Coercivity enhancement of hydrogenation–disproportionation–desorption–recombination processed Nd–Fe–B powders by the diffusion of Nd–Cu eutectic alloys, *Scr. Mater.* , 63 (2010) 1124-1127.
- [16] Z. Lin, J. Han, M. Xing, S. Liu, R. Wu, C. Wang, Y. Zhang, Y. Yang, J. Yang, Improvement of coercivity and thermal stability of anisotropic Nd₁₃Fe_{79.48}Nb_{0.3}Ga_{0.3} powders by diffusion of Pr–Cu alloys, *Appl. Phys. Lett.* , 100 (2012) 052409.
- [17] T. Sato, N. Oka, T. Ohsuna, Y. Kaneko, S. Suzuki, T. Shima, Enhancement of coercivity for Nd–Fe–B thin films by the infiltration of Nd–Cu alloy cap layer, *J. Appl. Phys.*, 110 (2011) 023903.
- [18] H. Nakamura, K. Hirota, T. Ohashi, T. Minowa, Coercivity distributions in Nd–Fe–B sintered magnets produced by the grain boundary diffusion process, *J. Phys. D: Appl. Phys* 44 (2011) 064003.

- [19] T. Akiya, J. Liu, H. Sepehri-Amin, T. Ohkubo, K. Hioki, A. Hattori, K. Hono, High-coercivity hot-deformed Nd–Fe–B permanent magnets processed by Nd–Cu eutectic diffusion under expansion constraint, *Scr. Mater.*, 81 (2014) 48-51.
- [20] F. Chen, T. Zhang, J. Wang, L. Zhang, G. Zhou, Coercivity enhancement of a Nd–Fe–B sintered magnet by diffusion of Nd₇₀Cu₃₀ alloy under pressure, *Scr. Mater.*, 107 (2015) 38-41.
- [21] H. Sepehri-Amin, Y. Une, T. Ohkubo, K. Hono, M. Sagawa, Microstructure of fine-grained Nd–Fe–B sintered magnets with high coercivity, *Scr. Mater.*, 65 (2011) 396-399.
- [22] C.D. Fuerst, J.F. Herbst, Hard magnetic properties of melt-spun Nd-Co-Fe-B materials, *J. Appl. Phys.*, 63 (1988) 3324.

Highlights

- Binder jetting additive manufacturing technique was employed to fabricate NdFeB isotropic bonded magnets.
- Printed magnets were infiltrated with low-melting point eutectic alloys [i.e., $\text{Nd}_3\text{Cu}_{0.25}\text{Co}_{0.75}$ (NdCuCo) and $\text{Pr}_3\text{Cu}_{0.25}\text{Co}_{0.75}$ (PrCuCo)].
- The printed magnet density was improved from 3.3 g/cm^3 to 4.3 g/cm^3 with infiltration.
- The intrinsic coercivity H_{ci} was enhanced from 732 to 1345 kA/m and 1233 kA/m after diffusion of NdCuCo and PrCuCo, respectively.